

Supporting Information

Exploration of proquinoidal [1,2,5]thiadiazolo[3,4-g]quinoxaline-based small molecule acceptor toward high-sensitivity shortwave infrared photodetection

Wei qi Zhang†, *Qingxia Liu*†, *Liu Yuan**, *Hanwen Zhang*, *Jiaqi Wang*, *Yang Wang**, *Yunxiang Deng*, *Yunhong Huang*, *Yadong Jiang* and *Huiling Tai**

1. Materials and methods

Materials:

All reagents were purchased from commercial sources without further purification. The donor **PTB7-Th** was purchased from 1-Material. Compound DTC-SnBu₃ is synthesized according to reported method.¹ Compound TQpp-2Br is purchased from Nanjing Zhiyan (<http://zhi-yan.cn/>).

Characterizations:

¹H, ¹⁹F and ¹³C NMR spectra were obtained on a Bruker DMX-400 NMR Spectrometer (using CDCl₃ as solvent) or Bruker AVIII 500WB NMR Spectrometer (using CDCl₂CDCl₂ as solvent). The chemical shifts were calibrated using solvent peak of tetramethylsilane as reference. The chemical shift was recorded in ppm and the following abbreviations were used to explain the multiplicities: s = singlet, d = doublet, t = triplet, m = multiplet, br = broad.

MALDI-TOF mass spectra were recorded on a Micromass GCT-MS spectrometer.

UV-vis-NIR absorption spectra were obtained with a SHIMADZU UV-3600i Plus spectrophotometer.

Cyclic voltammetry (CV) measurement was conducted on an electrochemical workstation with Pt disk coated with **TQpp** films, Pt plate, and Ag/Ag⁺ electrode as working electrode, counter electrode and reference electrode respectively, in a 0.1 mol L⁻¹ tetrabutylammonium phosphorus hexafluoride (Bu₄NPF₆) in acetonitrile solution. Redox potentials were internally calibrated using the ferrocene/ferrocenium (Fc/Fc⁺) redox couple (-4.8 eV).

Grazing-incidence Wide-Angle X-ray Scattering (GIWAXS) measurements were conducted on Xenocs-SAXS/WAXS system with X-ray wavelength of 1.5418 Å. The film samples were irradiated at a fixed angle of 0.2°. All film samples are prepared by spin-coating chloroform solutions on ZnO/silicon-wafer substrates.

Atomic force microscopy (AFM) images of the blend films were obtained from the devices directly on a VEECO Dimension 3100 atomic force microscope working under tapping mode. Transmission electron microscopy (TEM) images were obtained on a FEI Tecnai G2 F20 U-TWIN TEM instrument. Films spin-coated on ITO substrates under the same condition as the devices were immersed in water, and the floating active layers were transferred to TEM grid.

Quantum chemical calculations:

All calculations were performed with the Gaussian 16 program suite. In the calculations, the alkyl chains in the acceptor molecules were replaced by methyl groups for simplification. Full geometry optimizations were carried out at the B3LYP/6-31G(d, p) level, and the obtained stationary points were characterized by frequency calculations. The vibrational frequencies of the optimized geometries are all positive,

indicating that all the obtained geometries are stable. On the basis of the optimized geometries, excited-state calculations were performed by means of time-dependent DFT (TD-DFT). Vibrationally-resolved electronic spectra of the molecules were performed at B3LYP/6–31G(d, p) level using Franck-Condon approximation. TD-DFT calculations were conducted using the polarizable continuum model (PCM), taking the dielectric constant for chloroform as reference.

Space charge limited current (SCLC) measurement:

The hole and electron mobilities were measured by space charge limited current (SCLC) method with structures of ITO/PEDOT:PSS/active layer/MoO₃/Ag for hole-only devices and ITO/ZnO/active layer/PFN-Br/Ag for electron-only devices.

According to the Mott-Gurney square law:

$$J = 9\varepsilon_0\varepsilon_r\mu(V_{appl} - V_{bi} - V_s)^2/8L^3$$

where J is the current density, ε_0 is the vacuum permittivity, ε_r is the relative dielectric constant of the material (assumed to 3), μ is the electron or hole mobility, V_{appl} is the applied voltage, V_{bi} is the built-in voltage (0.2 V in this work), V_s is the voltage drop from the substrate's series resistance (0 V), and L is the thickness of the active layer film (~220 nm).

Fabrication and Characterization of OFETs:

The charge-transport properties of the SMAs were investigated by fabricating organic thin-film transistors with a with a top-contact/bottom-gate architecture. A heavily doped n-type Si wafer were employed as a gate electrode and dry oxidized SiO₂ (300 nm) were used as gate dielectric layer (capacitance per unit area of the dielectric

layer is 16.9 nF cm^{-2}). The Si/SiO₂ substrates were cleaned following by ultrasonication in sulfuric acid-hydrogen peroxide (H₂SO₄:H₂O₂ = 3:1), deionized water, and isopropyl. The Si/SiO₂ wafers were then dried under vacuum at 100°C for 1h. After that, 50 µl of OTS was dropped into a small petri dish placed next to the Si/SiO₂ wafers and heated to 100°C for 2h under vacuum condition. Then OTS treated Si/SiO₂ were ultrasonicated in chloroform and isopropyl successively. Then a 10 mg mL⁻¹ SMA solution in chloroform was spin-coated on the substrate at 2000 rpm for 30s. The gold drain and source electrodes of 80 nm in thickness were deposited on the devices under vacuum of $4 \times 10^{-6} \text{ Pa}$, defining device channels with the channel length and width of 100 µm and 50 µm, respectively. The electrical characteristics of SMA based OFET devices were measured in air using Keithley semiconductor analyzer (Keithley 4200-SCS). The mobilities were calculated from the saturation region with the following equation:

$$I_{DS} = (W/2L) C_i \mu (V_G - V_T)^2$$

where I_{DS} is the drain–source current, W is the channel width (100 µm), L is the channel length (50 µm), μ is the field-effect mobility, C_i is the capacitance per unit area of the gate dielectric layer, and V_G and V_T are the gate voltage and threshold voltage, respectively.

Photodetector Device Fabrication:

All photodiode devices are fabricated in inverted configuration of ITO/ZnO/active layer/MoO₃/Ag. ITO coated glass substrates were cleaned in deionized water, acetone and isopropyl alcohol for 10 min sequentially in ultrasonic bath. After dried in nitrogen

flow, the substrates were subjected to UV/ozone treatment for 15 min. Followed by the deposition of ~30 nm ZnO thin film by spin coating precursor solution onto the substrates at 4,000 rpm for the 40s and then annealing at 200°C for 30 min. The substrates were transferred into a glove-box with nitrogen atmosphere.

Active layer solutions (PTB7-Th:TQpp = 1:1 by weight) were prepared at a total concentration of 20 mg ml⁻¹ using chlorobenzene as solvent. The solutions were magnetically stirred overnight at 60°C in glove-box before spin coating. All the active layers were spin casted at 2,000 rpm in glove-box. At last, a MoO₃ layer (~10 nm) and Ag layer (~100 nm) were sequentially thermally evaporated under 10⁻⁴ Pa.

Device characterization:

The current-voltage characteristics were measured by Keithley 4200 semiconductor characterization system. The *R* and EQE spectra were carried out with a Keithley 2636B source meter under a 150-watt Xenon light source (Gloria-X150A) coupled with a monochromator, calibrated with a standard Si detector (S1337-1010BQ, Hamamatsu Photonics). The noise spectral density and response time were measured by PDA FS-Pro semiconductor parameter analyzer. The LDR was measured using a laser of 940 nm as the light source, while a series of filters were used to modulate the incident light intensity.

2. Synthesis Procedures

(1) Synthetic procedure for TQpp-2DTC:

To a flame-dried and N₂ filled three-neck round-bottom flask (50 mL) was added TQpp-2Br (1 mmol), DTC-SnBu₃ (1.90g , 2.75 mmol), Pd₂(dba)₃ (7.6 mg, 0.0083 mmol), P(o-tol)₃ (17.75 mg, 0.0583 mmol) and Toluene (15 mL). The flask was purged with N₂ for 10 min and followed by heating to 120 °C. After stirring for 24 h under 120 °C, the mixture was cooled to room temperature. Water (100mL) was added, and the mixture was extracted with dichloromethane (50 ml × 2), dried over Na₂SO₄ and concentrated in vacuum. The residue was purified by silica gel column chromatography (petroleumether) to afford the products. TQpp-2DTC was obtained as a deep green sticky solid (yield 75%). ¹H NMR (600 MHz, CDCl₃) δ 9.20 (d, J = 6.4 Hz, 2H), 7.87 – 7.78 (m, 4H), 7.48 (d, J = 5.8 Hz, 6H), 7.23 (s, 2H), 7.00 (dt, J = 5.3, 2.8 Hz, 2H), 2.08 (ddd, J = 12.4, 9.6, 3.1 Hz, 4H), 2.02 – 1.90 (m, 4H), 1.11 – 0.87 (m, 32H), 0.84 – 0.77 (m, 4H), 0.75 (t, J = 6.6 Hz, 6H), 0.65 – 0.54 (m, 18H). ¹³C NMR (151 MHz, CDCl₃) δ 158.06, 152.29, 138.21, 137.31, 134.69, 130.74, 129.39, 128.53, 128.28, 125.76, 120.86, 53.52, 43.42, 43.29, 35.26, 35.18, 34.29, 34.21, 28.67, 28.48, 27.37, 22.83, 14.10, 14.00, 13.97, 10.81, 10.61. MS (MALDI-TOF): calculated m/z 1141.77; found m/z 1140.08.

(2) Synthetic procedure for TQpp-2CHO:

A flame-dried and N₂ filled three-neck round-bottom flask (50 mL) was added with TQpp-2DTC (0.5 mmol), N,N-Dimethylformamide (3.86 mL, 50 mmol), and dry 1,2-dichloroethane (20 mL). The mixture was cooled to 0°C, and POCl₃ (2.29 mL, 25 mmol) was added dropwise during 15 min. After further reacting under ice-bath for 2h, the mixture was poured into ice water (200 mL), followed by adding saturated Na₂CO₃

solution (aq. 20 mL). After stirring for 1 h at RT, the mixture was extracted with dichloromethane (50 ml × 2), dried over Na₂SO₄ and concentrated in vacuum. The residue was purified by silica gel column chromatography (dichloromethane) to afford the products. TQpp-2CHO was obtained as a greenish brown solid (yield 96%). ¹H NMR (600 MHz, CDCl₃) δ 9.87 (s, 2H), 9.28 (dd, *J* = 7.9, 3.8 Hz, 2H), 7.81 (d, *J* = 7.1 Hz, 4H), 7.62 (t, *J* = 4.7 Hz, 2H), 7.53 (t, *J* = 7.1 Hz, 2H), 7.49 (t, *J* = 7.3 Hz, 4H), 2.17 – 2.08 (m, 4H), 2.06-1.97 (m, 4H), 1.08 – 0.89 (m, 32H), 0.80-0.72 (m, 10H), 0.66 – 0.54 (m, 18H). ¹³C NMR (151 MHz, CDCl₃) δ 182.51, 161.85, 159.01, 153.36, 151.84, 148.38, 143.89, 143.30, 141.42, 137.72, 135.05, 130.73, 129.92, 128.60, 128.45, 121.34, 54.03, 43.29, 43.19, 35.42, 35.35, 34.46, 34.13, 28.64, 28.43, 27.66, 27.36, 22.80, 22.76, 14.08, 13.97, 13.94, 10.78, 10.61. MS (MALDI-TOF): calculated *m/z* 1197.79; found *m/z* 1196.09.

(3) Synthetic procedure for TQpp:

To a flame-dried and N₂ filled three-neck round-bottom flask (50 mL) was added TQpp-2CHO (0.5 mmol), BF₃·Et₂O (0.62 mL, 5 mmol), 2-(5,6-difluoro-3-oxo-2,3-dihydro-1H-inden-1-ylidene)malononitrile (288 mg, 1.25 mmol), acetic anhydride (0.5 mL) and toluene (30 mL). After stirring for 1.5 h under RT, the mixture was poured into methanol (300 mL) under stirring. The precipitate was collected, washed with methanol several times, then recrystallized in chloroform:methanol mixed solvents to get the pure products. TQpp was obtained as a dark blue solid (yield 92%). ¹H NMR (400 MHz, CDCl₃) δ 9.39 (d, *J* = 2.5 Hz, 2H), 8.91 (s, 2H), 8.53 (dd, *J* = 9.9, 6.5 Hz, 2H), 7.80 (dd, *J* = 7.5, 1.6 Hz, 4H), 7.69 (t, *J* = 7.5 Hz, 4H), 7.58 (q, *J* = 4.5 Hz, 6H),

2.21-2.11 (m, 4H), 2.11 – 1.95 (m, 4H), 1.11 – 0.87 (m, 32H), 0.85-0.77 (m, 4H), 0.73 (t, $J = 6.4$ Hz, 6H), 0.70 – 0.53 (m, 18H). ^{19}F NMR (376 MHz, CDCl_3) δ -123.77 (d, $J = 19.2$ Hz), -124.96 (d, $J = 19.1$ Hz). MS (MALDI-TOF): calculated m/z 1622.10; found m/z 1621.70.

Reference:

1. B. P. Karsten, J. C. Bijleveld, L. Viani, J. Cornil, J. Gierschner and R. A. J. Janssen, *J. Mater. Chem.*, 2009, **19**, 5343-5350.

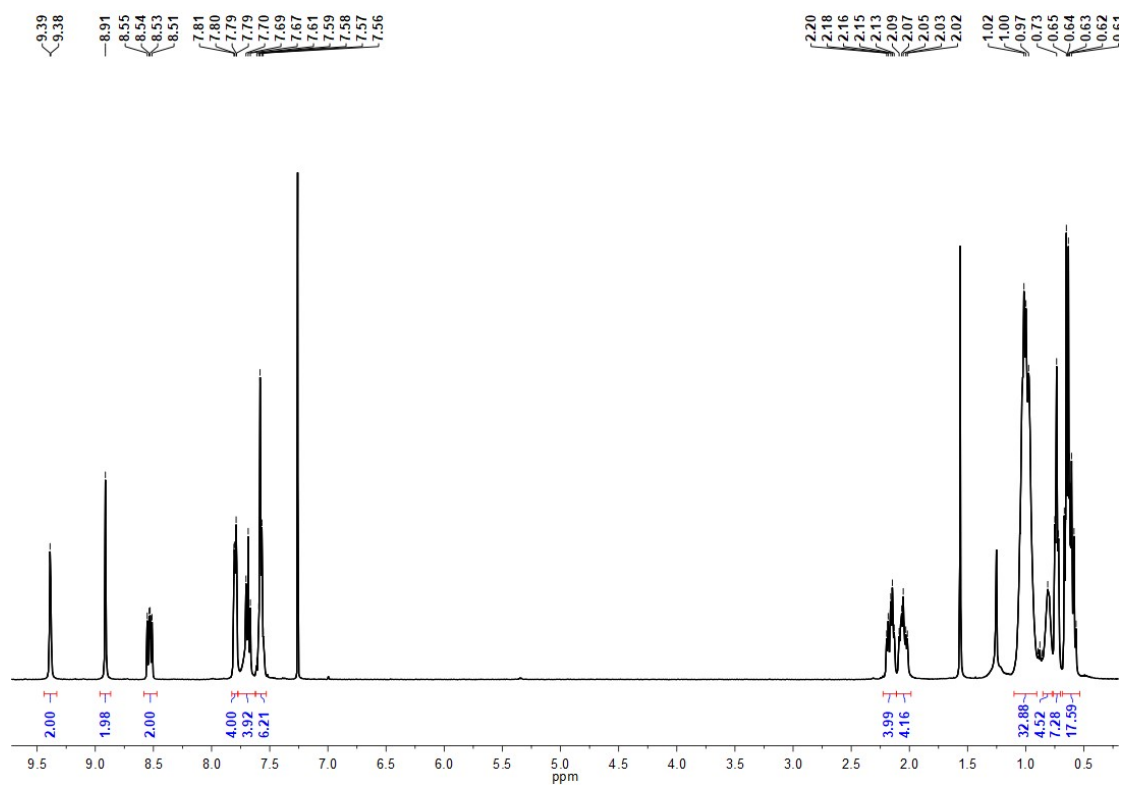


Fig. S1 $^1\text{H-NMR}$ of TQpp (400 MHz, CDCl_3).

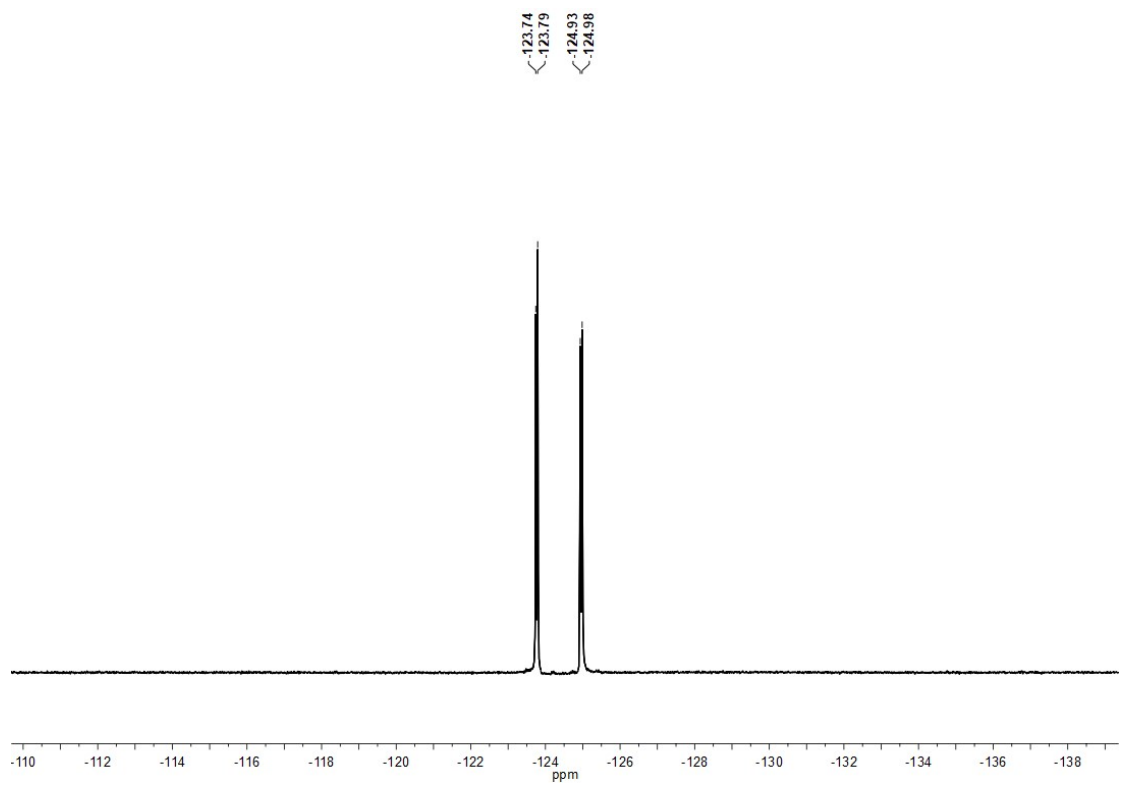


Fig. S2 $^{19}\text{F-NMR}$ of TQpp (376 MHz, CDCl_3).

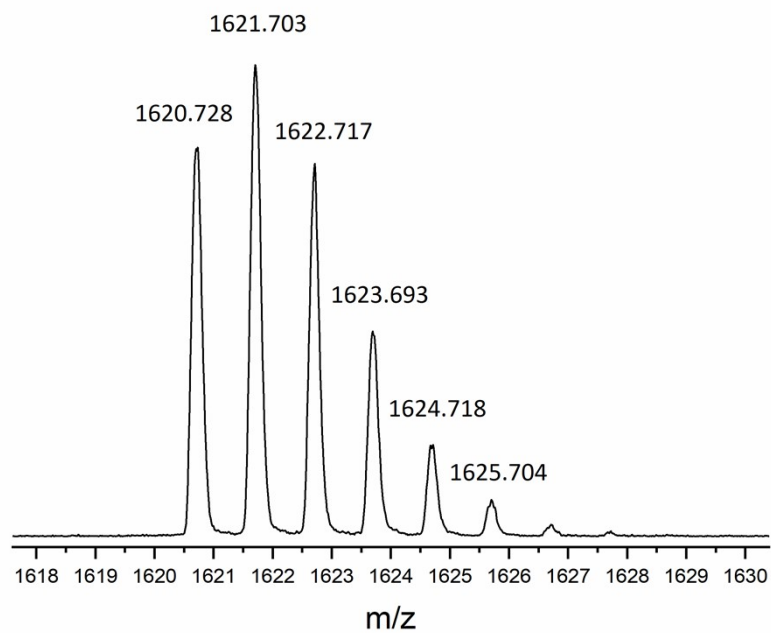


Fig. S3 MALDI-TOF mass spectrum of TQpp.

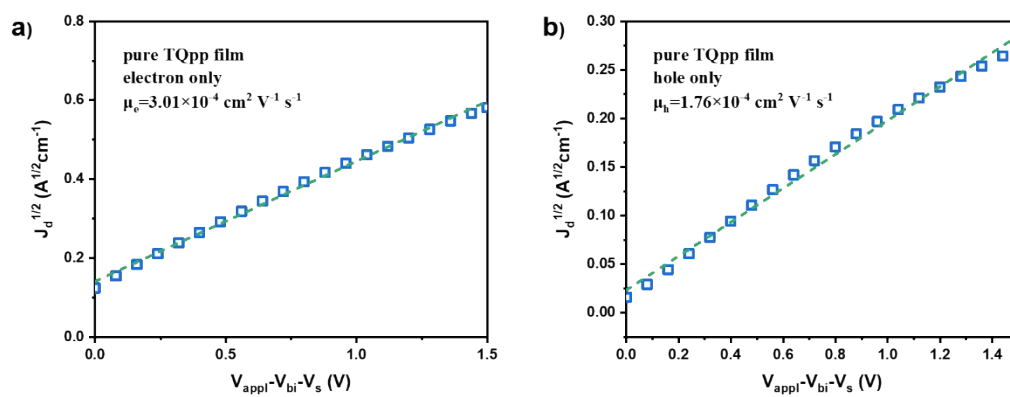


Fig. S4 $J^{1/2}$ -V characteristics of a) electron-only and b) hole-only devices of pure TQpp film for carrier mobility measurement through SCLC method.

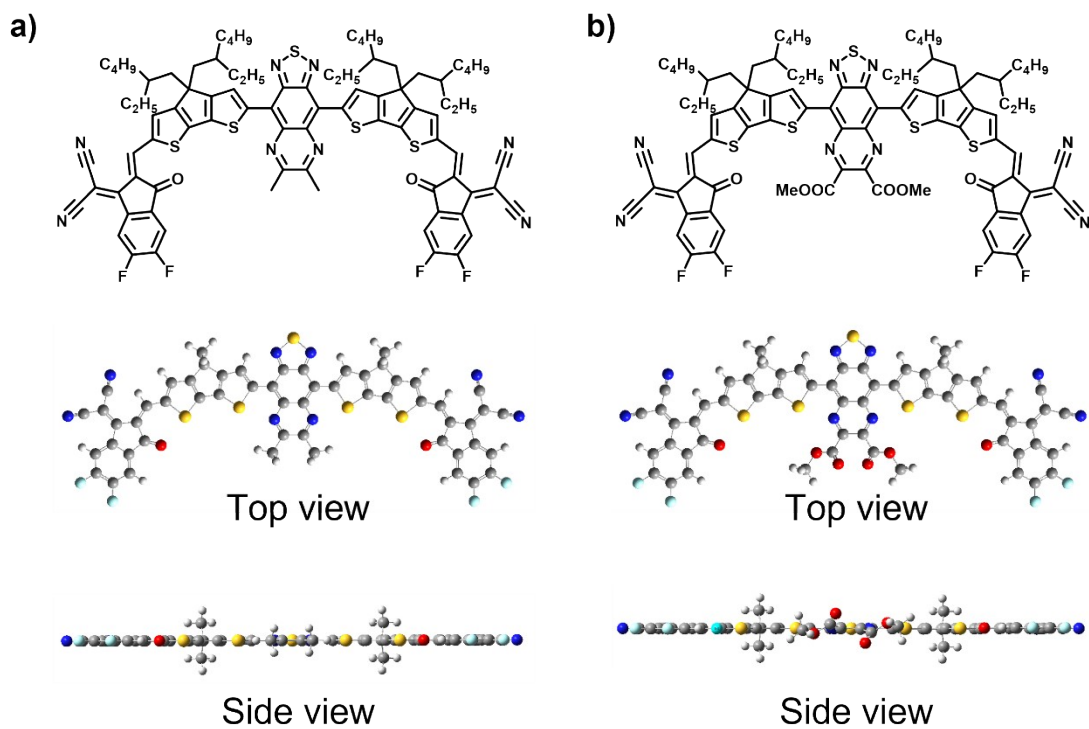


Fig. S5 Top view and side view of optimized geometry for TQpp's a) alky and b) ester substitution analog calculated at the B3LYP/6-31G(d, p) level.

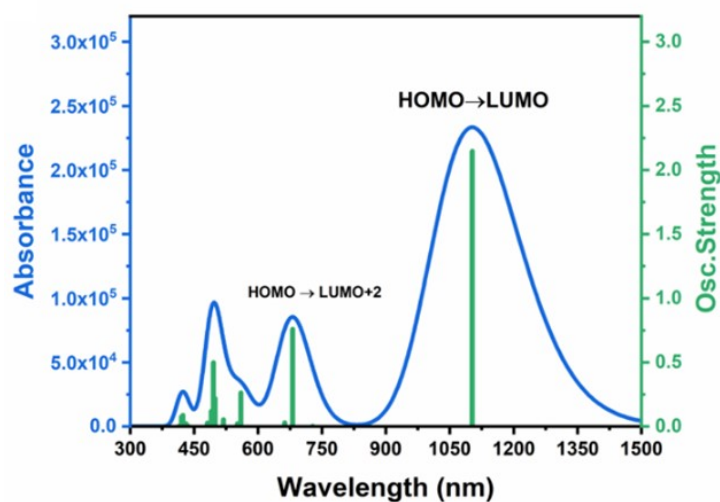


Fig. S6 TD-DFT calculated absorption spectra of TQpp at the B3LYP/6-31G** level of theory.

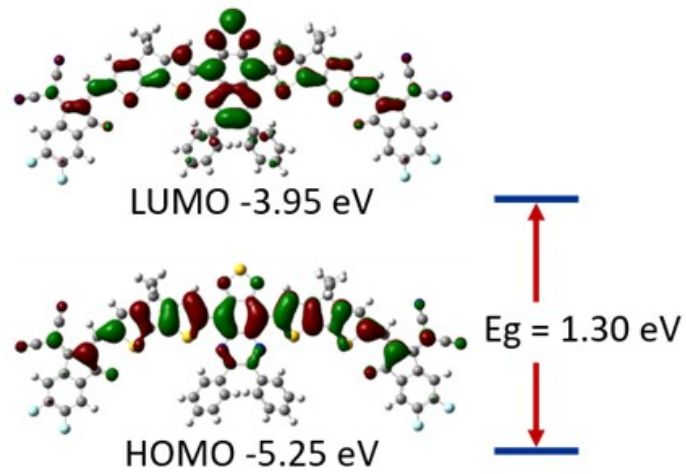


Fig. S7 DFT calculated frontier orbitals, energy levels and band-gap of TQpp.

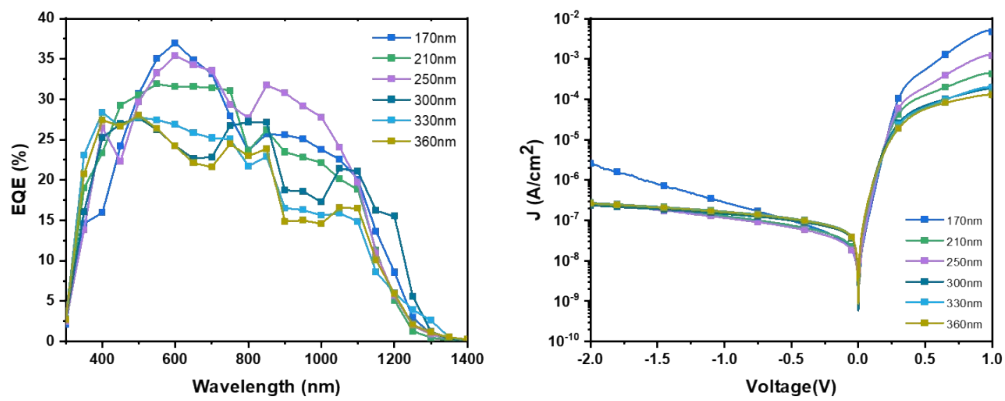


Fig. S8 a) EQE and b) J - V curves in dark with different active layer thickness.

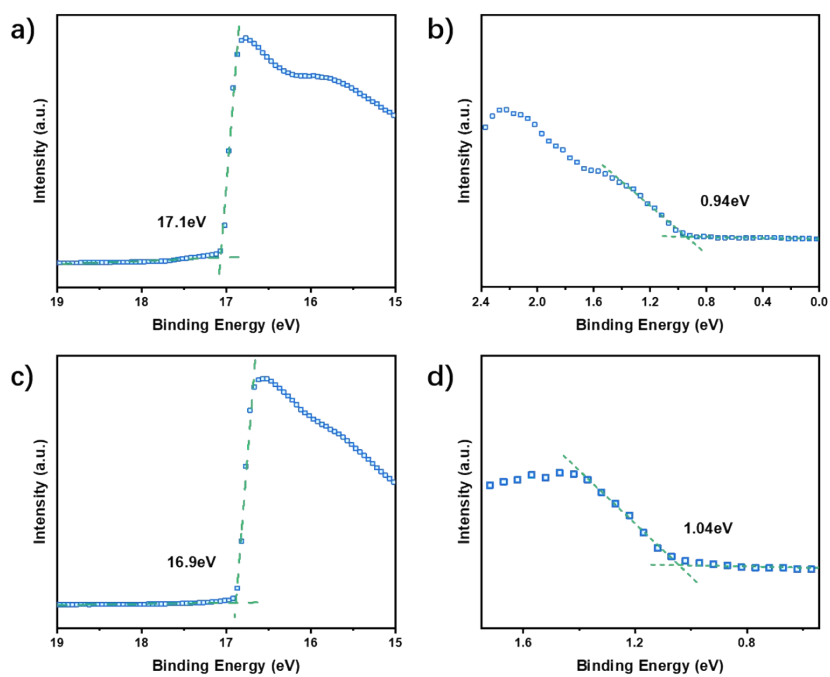


Fig. S9 UPS secondary electron cut-off of a) PTB7-Th and c) TQpp. Fermi edge of b) PTB7-Th and d) TQpp.

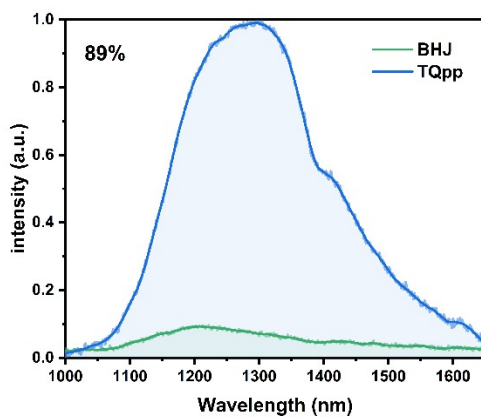


Fig. S10 Photoluminescence (PL) spectrum for TQpp film and BHJ film.

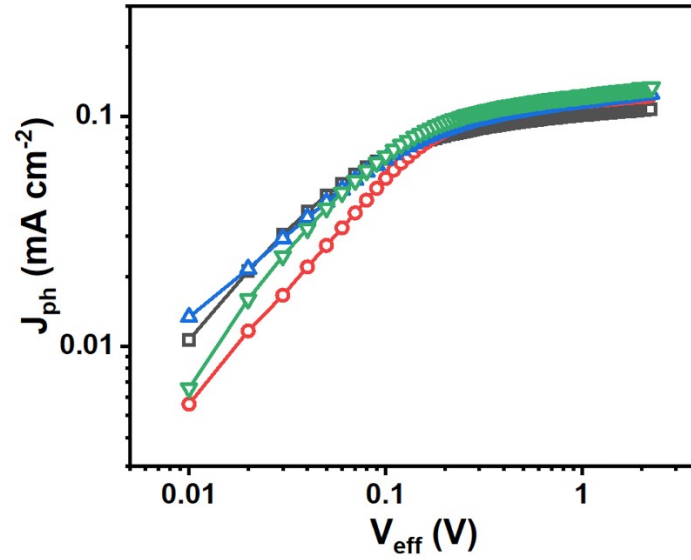


Fig. S11 J_{ph} - V_{eff} characteristics of four ITO/ZnO/TQpp:PTB7-Th/MoO₃/Ag-based devices measured under 1100 nm irradiation with power density of 0.475 mW cm⁻².

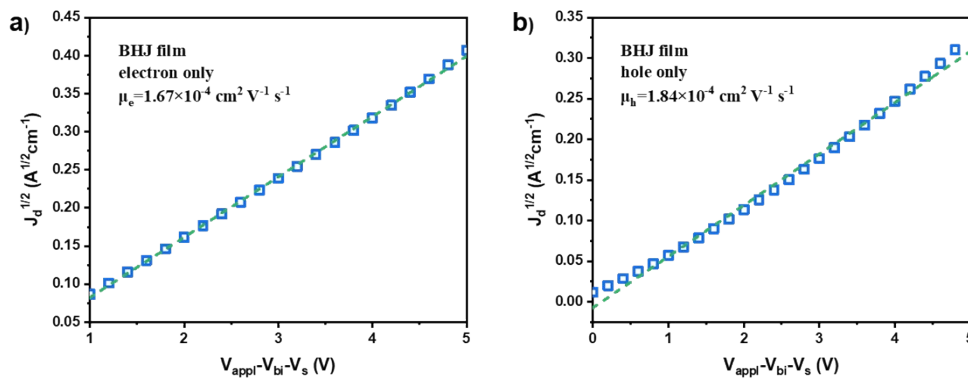


Fig. S12 $J^{1/2}$ - V characteristics of a) electron-only and b) hole-only devices of BHJ film for carrier mobility measurement through SCLC method.

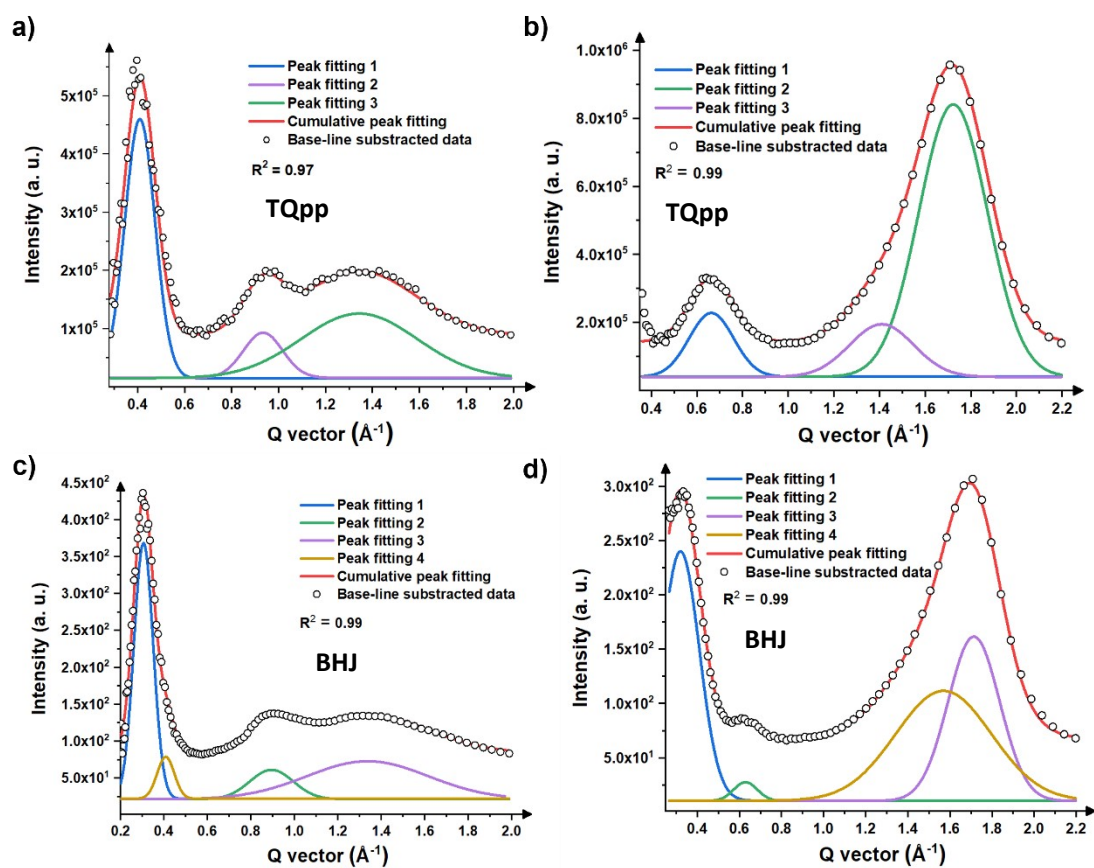


Fig. S13 Gaussian fitting for GIWAX a, c) in-plane cut and b, d) out-of-plane cut.

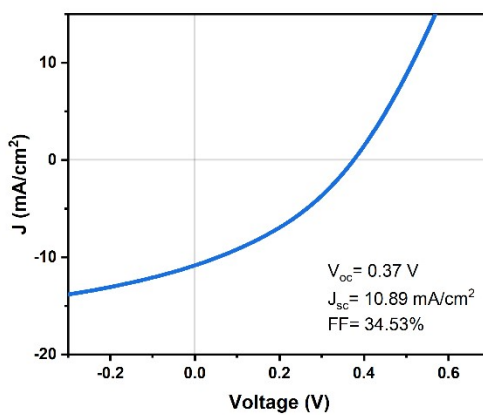


Fig. S14. The typical current density-voltage characteristics of ITO/ZnO/TQpp:PTB7-Th/MoO₃/Ag-based devices measured under simulated AM 1.5G irradiation.

Table S1 Summary of GIWAXS scattering patterns of the pure TQpp film and BHJ film.

	In-plane				Out-of-plane			
	q_{xy} [\AA^{-1}]	d [nm]	FWHM	CCL [nm]	q_z [\AA^{-1}]	d [nm]	FWHM	CCL [nm]
TQpp	0.41	1.53	0.15	3.77	0.66	0.95	0.23	2.46
	0.93	0.68	0.20	2.83	1.41	0.45	0.33	1.71
	1.34	0.47	0.58	0.97	1.72	0.37	0.35	1.61
TQpp-BHJ	0.31	2.02	0.11	5.14	0.32	1.96	0.21	2.69
	0.41	1.53	0.09	6.28	0.63	1.00	0.13	4.35
	0.90	0.70	0.24	2.36	1.57	0.40	0.54	1.05
	1.34	0.47	0.66	0.86	1.71	0.37	0.29	1.95